

## Closure behaviour of small cracks

Günter Ebi and Peter Neumann

Measurements of the initiation, growth, and closure behaviour of micro-cracks are reported for one ferritic and one austenitic low strength steel. Interferometric measurements of the COD of small surface cracks were performed with a resolution of 3 nm in order to measure the closure behaviour of micro-cracks. The van der Waals forces between atoms were added numerically in order to calculate the normal as well as the tangential forces acting between closely separated crack faces. The results are discussed in the context of the growth and closure of micro-cracks.

**Schließverhalten von Mikrorissen.** Es wird über Messungen der Bildung, der Ausbreitung und des Schließverhaltens von Mikrorissen in einem ferritischen und in einem austenitischen Stahl berichtet. Dazu wurden interferometrische Messungen der Rissöffnung von keinem Oberflächenrissen mit einer Auflösung von 3 nm durchgeführt. Die Van-der-Waals-Wechselwirkung zwischen Atomen wurde numerisch aufaddiert, um die Normal- und die Tangentialkraft zwischen den Rissufern beim Riss schließen zu berechnen. Die Resultate werden im Zusammenhang mit dem Wachstum und dem Schließverhalten von Mikrorissen diskutiert.

The fatigue life of many engineering alloys is dominated by the growth of surface micro-crack<sup>1)–3)</sup>. Short cracks generally grow faster than long cracks when subjected to the same nominal driving force. In the literature various hypotheses have been put forward in order to explain the anomalous growth behaviour of small fatigue cracks: absence of crack closure, plasticity effects, interaction with the micro-structure and geometrical effects. In the present study emphasis was placed on the local measurement of the cyclic crack opening displacement by means of high resolution interference technique. From these measurements the crack closure behaviour was determined and its influence on the small crack effect assessed separately from other parameters.

### Experimental

The materials chosen for this investigation were an austenitic stainless steel (German grade X6CrNi1811) and a mild steel (German grade St 37) having a monotonic yield stress of 220 MPa and 234 MPa, respectively. For all experiments smooth tensile specimens were employed, the gauge sections being 16 mm long and 8 mm in diameter. Constant amplitude tests were done under plastic strain and mean stress control. The cracks were allowed to initiate naturally by fatigue and their growth was monitored by replicating the gauge section periodically (time period < 0.05 Nf). The surface micro-cracks have a well defined almost semi-circular shape with a ratio of crack depth to surface crack length of 0.45 which agrees with finite element calculations of the local stress intensity along the front of thumbnail surface cracks<sup>4)</sup>. Most of the crack

depth data in this study were obtained by multiplying the measured surface crack length by 0.45.

The closure level of the micro-cracks has been determined from the measurement of the crack opening displacement (COD) as a function of the applied load. The determination of the COD of surface micro-cracks has been accomplished by using an interferometric displacement gauge according to Sharper). In order to record the change in the local crack deformation behaviour throughout the test about 50 µm sized cracks were initiated in the austenitic stainless steel and marked by micro-hardness indentations. During the test loading cycles with a frequency of 0.01 Hz were introduced at regular intervals in order to measure the local load displacement curve.

### Results and discussion

**Micro-crack growth.** There is a continuous crack propagation in X 6 CrNi 1811. Crack tips which approach a grain boundary at the surface are not retarded. This behaviour is typical for all cracks observed in the austenitic material. In contrast to the austenitic steel grain boundaries in mild steel represent strong barriers to micro-crack growth since the cracks exhibit a typical stop and go behaviour. This has also been observed by other investigators in mild steel<sup>6)</sup> and pure iron specimens<sup>7)</sup>. The cracks initiate in slip bands preferentially oriented parallel to a grain boundary and their growth temporarily stops when they hit the first boundary. The time for crack nucleation and growth within the first surface grain takes 15-25% of the total life, Nf, whereas slip bands are visible after 1 % of Nf. When the crack continues to propagate into the neighbouring grains and approaches the second neighbour boundaries another crack arrest occurs. Finally, after 40-45% of Nf the micro-cracks exhibit a continuous propagation behaviour throughout the rest of the fatigue life.

The surface observations indicate that the early stages of small crack behaviour are a direct consequence of the nucleation mechanism. In mild steel the cracks initiate in slip bands. Therefore, the entire crack is restricted to one surface grain. Although, this grain is oriented favourably to the stress axis by the very nature of the initiation process this is generally not true for neighbouring grains. There-

Information from the Max-Planck-Institut für Eisenforschung GmbH, paper No. 1549.

This paper was presented as a keynote lecture at the Internal. Conference on Fatigue and Fatigue Threshold in the Pacific Basin, Fatigue 90, July 16, 1990, Honolulu, Hawaii.

Authorized reprint from Proc. Fatigue 90. Published by Materials and Component Engineering Publications LTD., Birmingham, U. K. Dr.-Ing. Günter Ebi (now with SENSOPLAN GmbH, Hohentengen, Germany) during this investigation assistant scientist; Prof. Dr. rer. nat. Peter Neumann, Dept. of Physical Metallurgy, Max-Planck-Institut für Eisenforschung GmbH, Düsseldorf, FRG.

fore, a further nucleation process has to take place which carries the crack across the boundary. On the other hand, cracks in austenitic stainless steel nucleate at twin boundaries or even grain boundary triple points. In this case the crack front cuts two or three differently oriented grains from the very beginning. Therefore, a time consuming takeover into the first neighbours will not occur due to the nature of the initiation site.

Since the small cracks in ductile steels are embedded in a fully plastified specimen, linear fracture mechanics are not applicable for the rationalization of the growth data. For such a case the cyclic J-integral<sup>8)</sup> is the appropriate parameter which we shall call Z in order to distinguish it from the monotonic I Integral. For thumbnail cracks Z is given by

$$Z = a \left( 1.45 \frac{\Delta\sigma^2}{E} + \frac{2.4}{\sqrt{1+3n}} \Delta\sigma \Delta\varepsilon_p \right), \quad (1)$$

E is Young's modulus, n the strain hardening exponent. For long cracks Z is obtained from the relation

$$Z = \frac{1-\nu^2}{E} \Delta K^2. \quad (2)$$

The growth rates of the micro-cracks in the austenitic stainless steel are plotted versus Z in figure 1. For comparison own growth data of long fatigue cracks in CT-specimens and published data of Rieux et al.9) (SEN-specimens) are also included. The use of Z reduces the scatter of this data set, however, at small amplitudes only cracks greater than 160  $\mu\text{m}$  show a power law correlation between da/dN and Z. Below 160  $\mu\text{m}$ , which is about three times the grain size, the fast growth is observed.

**Micro-crack closure.** The fast growth behaviour of surface micro-cracks is very often attributed to the absence of a premature closure of the crack surfaces. The idea is that small fatigue cracks are free of fracture surface roughness or plastic wake. For long fatigue cracks both effects reduce the crack opening displacement and, therefore, cause a premature contact of the crack flanks. In order to test the validity of this hypothesis the relative movement of the crack mouth was recorded with the Sharpe technique with a resolution of 3 nm as a function of the load in order to check for signs of closure. The closure experiments were performed with the austenitic steel using a plastic strain amplitude of  $5 \times 10^{-4}$ .

**Figure 2** shows a typical example of a load-displacement curve of a micro-crack. The symbols represent data points that have been measured by means of the interference technique. In these local hysteresis loops closure shows up in two ways: first, there is a strong non-linearity before the lower reversal point and second, the elastic slopes after the upper and lower reversal points are different. The closure stress was evaluated from the local hysteresis according to Bowling and Begley<sup>10)</sup>. The procedure is shown in figure 2. The slope of the hysteresis after the lower reversal point corresponds to the Young's modulus of the uncracked austenitic material. This means, that the crack flanks are in contact and stay together. However, the steep slope extends beyond the closure stress level. Similar observations are reported by Rie and Schubert<sup>11)</sup> and Iyyer and Dowling<sup>12)</sup>. This suggests that the opposing fracture surfaces stick together even above the closure stress level, i.e. tensile forces

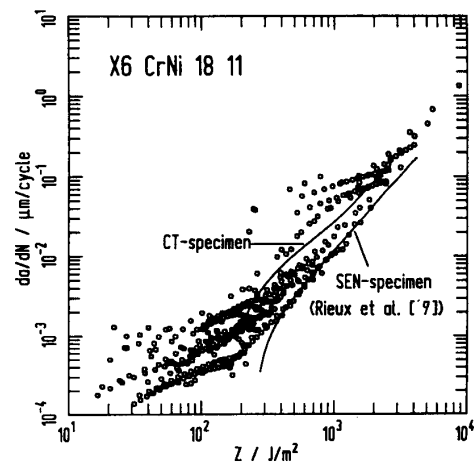


**Figure 1.** Growth rate of short (symbols) and long (lines) fatigue cracks as a function of the Z Integral (austenitic steel)

**Bild 1.** Rissausbreitungsgeschwindigkeit kurzer (Symbole) und langer (Linien) Ermüdungsrisse als Funktion des Z Integrals (austenitischer Stahl)

are transmitted across the crack. When the same microcrack is loaded with a tensile mean stress of 50 MPa, the lower reversal point is raised to the previous closure level, closure disappears and a perfect symmetric hysteresis loop is observed, **figure 3**.

The closure behaviour of the micro-cracks expressed as

$$U = \frac{\sigma_{\max} - \sigma_{\text{cl}}}{\sigma_{\max} - \sigma_{\min}} \quad (3)$$

is plotted in figure 4 as a function of crack length. For cracks smaller than 120  $\mu\text{m}$  a premature closure cannot be observed and  $U = 1$ . In the range  $120 \mu\text{m} \leq a \leq 600 \mu\text{m}$

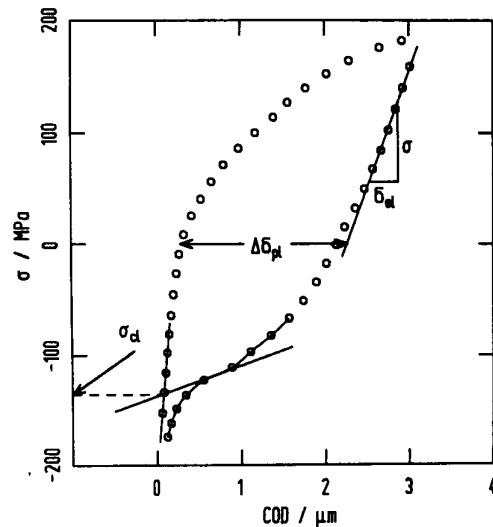


**Figure 2.** Local load-displacement hysteresis of a microcrack ( $a = 274 \mu\text{m}$ ) and definition of closure stress (austenitic steel)

**Bild 2.** Lokale Kraftverschiebungshysteresis eines Mikrorisses ( $a = 274 \mu\text{m}$ ) und Definition der Risschließspannung (austenitischer Stahl)

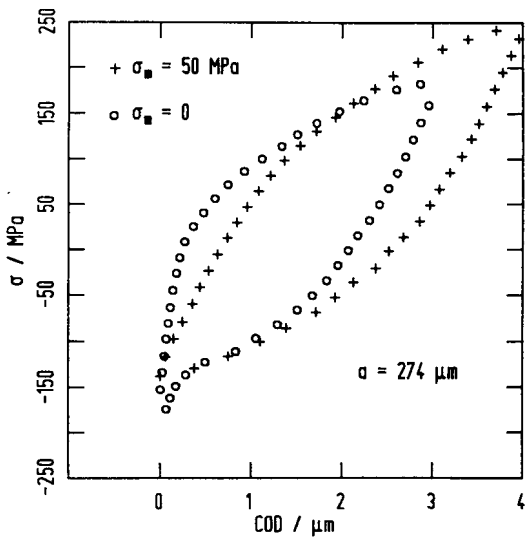


**Figure 3.** Influence of the mean stress on the shape of the local hysteresis loop (austenitic steel)

**Bild 3.** Einfluss der Mittelspannung auf die Gestalt der lokalen Hysterese (austenitischer Stahl)

$U$  decreases continuously and reaches a constant value of 0.82 at  $a = 600 \mu\text{m}$ . Physically, this result expresses the fact that the crack stays open for most of the compressive phase. Since loading has been performed at  $R = -1$ , this observation contradicts the widespread opinion that cracks are always closed in the compressive part of the load cycle.

In general, the opposing crack surfaces contact when  $\text{COD} = 0$ . If one assumes for the moment a crack which is free of roughness and plastic wake then it is possible to predict the contact load from continuum mechanics arguments. For small scale yielding (ssy) situations Rice<sup>13)</sup> estimated that the opposing fracture surfaces touch each other when the stress variation  $\Delta\sigma$  exceeds the maximum applied stress  $\sigma_{\text{max}}$  by only a few percent. Thus, for fully reversed loading, the crack essentially remains closed during the compressive phase and only the tensile portion of the load cycle contributes to crack growth.

For general yield, as in the low strength steels considered here, the situation is different. If crack closure occurs, it always introduces a tensile mean stress locally at the crack tip, in spite of the fact that the specimen is loaded with  $R = -1$ . Under general yield conditions this will lead to cyclic creep and stress relaxation at the crack tip, because there is no surrounding elastic zone. This will open up the crack until closure does not occur at all or just at the lower reversal point. Then the local stresses are symmetric and cyclic creep stops.

Hence, for an ideal crack, closure occurs under general yield conditions subject to cyclic creep at  $\sigma_{\text{min}}$  and at  $\Delta\sigma/\sigma_{\text{max}} = 1.1$  under ideal ssy conditions. In fact, the closure measurements performed on small fatigue cracks in high-strength Al-alloys<sup>14)-16)</sup> and Ti-alloys<sup>17)</sup> yield closure stresses which considerably exceed the values estimated by Rice<sup>13)</sup>. According to Suresh and Ritchie<sup>18)</sup> fracture surface roughness, plastic wake effects and oxidation of the crack flanks raise the closure stress because they reduce the COD. In the present study oxide induced closure can be discarded since the tests have been performed with a stainless steel in ambient air. The influence of plastic wake on crack closure behaviour has been modelled by

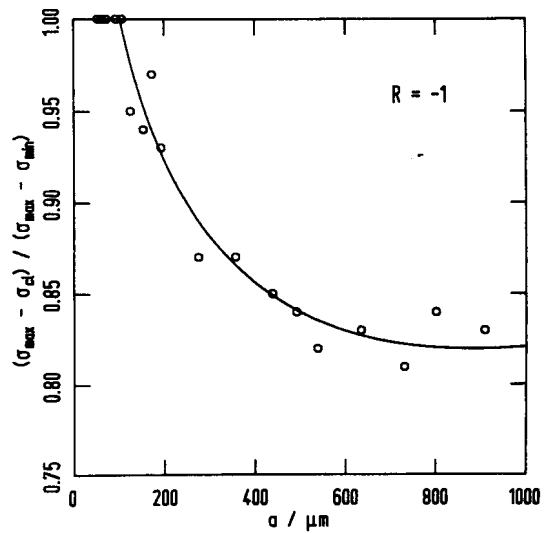


**Figure 4.** Normalized opening stress range as a function of crack length  $a$  (austenitic steel)

**Bild 4.** Riss-schließverhalten als Funktion der Risslänge  $a$  (austenitischer Stahl)

Budiansky and Hutchinson<sup>19)</sup>. Their analysis is based on plane stress conditions. For this case one can think of a plastic material flow from the necked specimen surface to the crack flanks so that the volume is retained. However, for semi-circular surface cracks one would rather expect plane strain conditions. Therefore, the analysis of Budiansky and Hutchinson does not apply.

The only remaining possibility is that fracture surface roughness is responsible for premature crack closure in the present investigation. If this hypothesis is correct, cracks longer than  $160 \mu\text{m}$ , which show premature closure, should have a surface-COD  $> 0$  even at maximum compression and shorter ones should be closed then (surface-COD = 0). In order to check this, cracks were replicated at the lower reversal point. The results are shown in **figure 5**, which demonstrates quite convincingly that prematurely

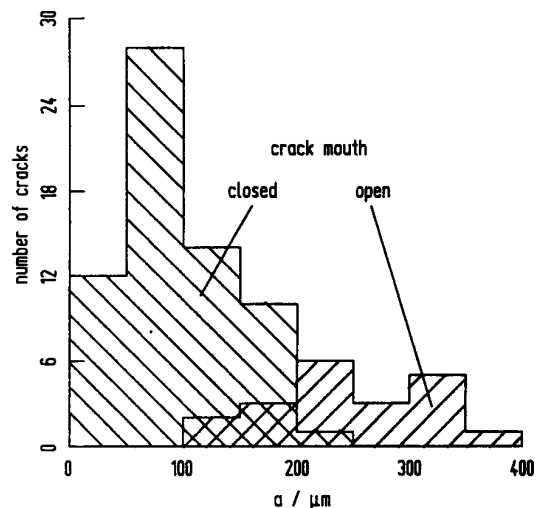


**Figure 5.** Histogram of lengths of cracks with surface-COD = 0 or  $> 0$  at  $\sigma = \sigma_{\text{min}}$  (austenitic steel)

**Bild 5.** Histogramm der Risslängen mit Oberflächenrissöffnung = 0 oder  $> 0$  bei  $\sigma = \sigma_{\text{min}}$  (austenitischer Stahl)

closing cracks have a non-vanishing surface-COD even at maximum compression. This strongly favours fracture surface roughness as the responsible mechanism for crack closure.

With the data of figure 4 at hand, the effect of crack closure on crack growth can be accounted for by calculating an effective  $Z$  in analogy to  $\Delta K_{\text{eff}} = U \cdot \Delta K$  under ssy conditions. Since  $Z \propto \Delta K^2$  we write:

$$Z_{\text{eff}} = U^2 \cdot Z. \quad (4)$$

The effective  $Z$  integral was determined from the measured  $U(a)$  relation and the  $da/dN$  curve is replotted in terms of  $Z_{\text{eff}}$  for the tests with  $\Delta \epsilon/2 = 5 \cdot 10^{-4}$  in figure 6. Even in this  $Z_{\text{eff}}$ -plot the faster growth of short crack lengths is clearly visible. Hence, for the austenitic stainless steel the short crack effect cannot be explained to its full extent by the absence of crack closure. It is obviously due to the fact that cracks always nucleate at exceptionally well suited places, at which also early crack growth is favoured. Only after about three grain diameters the average environment is encountered and average crack growth takes place.

### A new mechanism of crack closure: van der Waals interaction of crack faces

**Normal stresses.** The great difference between the closing and opening stress as measured locally at micro-cracks is a direct evidence of sticking forces acting between the crack faces. Well known mechanisms for such interaction forces are - rewelding of the crack faces<sup>20</sup>), - interlocking crack faces<sup>21</sup>).

Here, a new mechanism is proposed employing van der Waals interaction forces. This mechanism is rather attractive because it supplies some clues explaining, why small cracks first propagate as shear cracks (stage I) and why they switch to mode I cracks during the later stage II only.

The van der Waals interaction is usually regarded as short ranged, since the interaction potential between two atoms is proportional to  $d^{-6}$ , where  $d$  is the distance between the atoms:

$$\omega_{\text{atoms}} = -\frac{C}{d^6}. \quad (5)$$

Two crack faces are described best, however, as two half spaces at a mutual distance,  $D$ , from each other. In order to calculate their van der Waals interaction, the contributions of all the atoms involved have to be added. In a continuum approximation the summation may be replaced by an integration, which can be carried out analytically for two opposing half spaces at a mutual distance,  $D$ . The result is

$$\omega_{\text{half-spaces}} = -\frac{A}{12\pi d^2} \quad (6)$$

with

$$A = \pi^2 \cdot C \cdot \left( \frac{\text{atoms}}{\text{volume}} \right)^2 \quad (7)$$

which is rather long-ranged, indeed. The coefficient,  $A$ , is known as the Hamaker constant<sup>22</sup>) and has a value of  $4 \times 10^{-19}$  J for most metals. The resulting attractive force

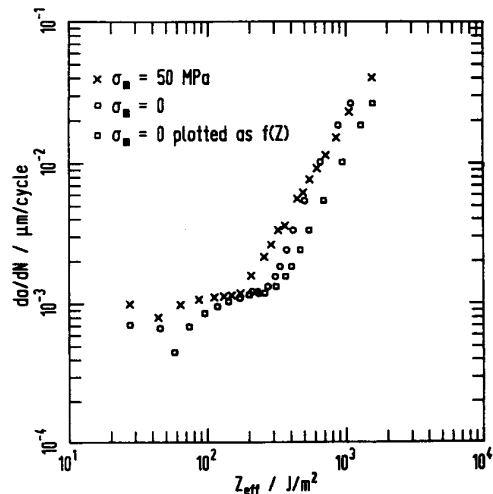


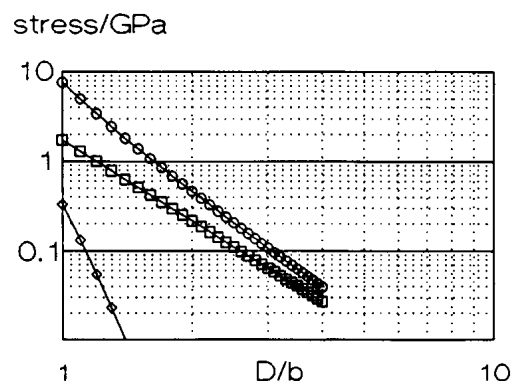
Figure 6. Growth rate of micro-cracks as a function of  $Z_{\text{eff}}$  (austenitic steel)

Bild 6. Ausbreitungsgeschwindigkeit von Mikrorissen als Funktion von  $Z_{\text{eff}}$  (austenitischer Stahl)

per area, the continuum van der Waals stress,  $\sigma_{\text{cont}}$ , is

$$\sigma_{\text{cont}} = \frac{A}{6\pi d^3}. \quad (8)$$

It is shown in figure 7 as a function of the distance  $D$ , measured in units of the lattice spacing  $b = 0.23$  nm ( $A = 4 \times 10^{-19}$ , one atom/ $b^3$ ). Figure 7 indicates that considerable stresses can be transmitted across cracks which are only a few lattice spacings wide. Thus, due to the van der Waals forces a closed crack opposes the re-opening up to the point, where the applied stress exceeds the van der Waals stress. Calculation of  $\sigma_{zz}$  requires the distribution of  $D$ -values across the closed crack, which is largely unknown. The range of stress shown in figure 7 is, however,



- squares:  $\sigma_{zz}$  between continua,
- circles:  $\sigma_{zz}$  of discrete model,
- diamonds:  $\sigma_{xz}$  of discrete model
- Quadrate:  $\sigma_{zz}$  zwischen Kontinua,
- Kreise:  $\sigma_{zz}$  des diskreten Modells,
- Rauten:  $\sigma_{xz}$  des diskreten Modells

Figure 7. Van der Waals stresses between half-spaces vs their distance:

Bild 7. Van-der-Waals-Spannungen zwischen zwei Halbräumen in Abhängigkeit von deren gegenseitigem Abstand

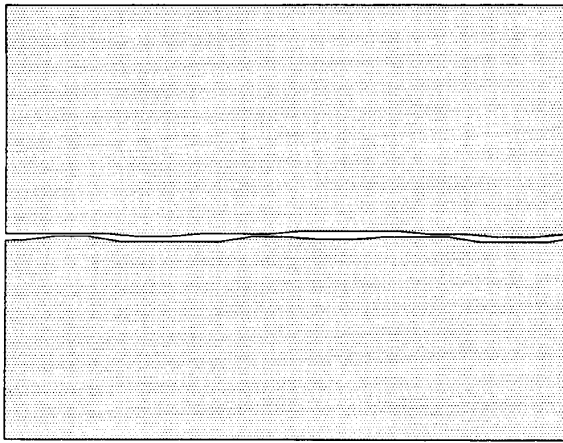


**Figure 8.** Possible geometry of a closed crack. Contact areas alternate with areas of small separation. Thus, a large fraction of the interacting forces is of the van der Waals type

**Bild 8.** Mögliche Geometrie eines geschlossenen Risses. Berührungsstellen wechseln ab mit Flächen geringen Abstands. Daher ist ein Großteil der Wechselwirkungskräfte von der Art der Van-der-Waals-Kräfte

of the appropriate magnitude to account for the observed difference between the closing and the opening stress of micro-cracks (cf. figures 2, 3).

The idealized configuration of two opposing half-spaces is not very realistic for a closed crack. In addition it should be noted that ideal half spaces kept apart under force boundary conditions are at an unstable equilibrium at any value of  $D$ , since the interaction forces are decreasing with increasing  $D$ . In reality there will be contact areas scattered over the crack surface with areas of small separation of the crack faces in between, as shown in **figure 8**. The point is, that also in this more realistic scenario a large fraction of the interacting forces will be of the van der Waals type

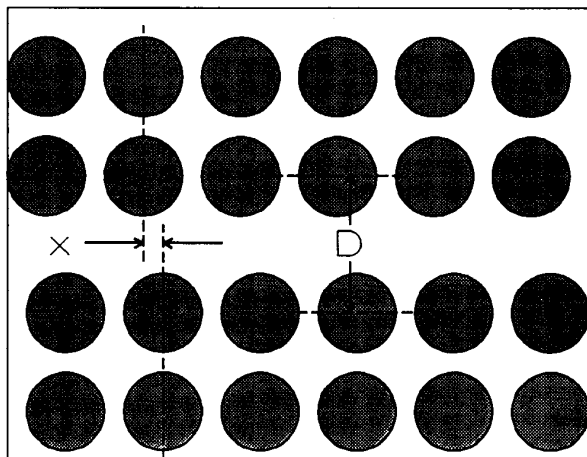


**Figure 9.** Atomistic structure of crack faces with the definition of  $x$  and  $D$ ;  $y$  is defined correspondingly

**Bild 9.** Atomistische Struktur der Rissflächen mit Definition  $x$  and  $D$ ;  $y$  ist entsprechend definiert

because a perfect contact over the whole crack surface is unlikely.

**Shear stresses.** In the continuum model it is obvious that only normal stresses, opposing mode I opening of the crack faces, are generated by the van der Waals interaction. This hinders mode I opening of the crack. However, any mode II or III displacement of the crack faces is not hindered by the van der Waals interaction. Therefore, the reduction of the local stress intensity due to van der Waals forces holds only for mode I but not for mode II or III. This bears a reason for the often observed stage I propagation mode. Small crack nuclei along slip planes, which are rather flat, can be modelled by a situation as shown in **figure 8**, which implies that such cracks would preferentially grow in mode II or III.

This line of arguments uses the fact that in a continuum model of the van der Waals interaction no shear forces are transmitted from one crack face to the other. If, however, the discrete atomistic situation as shown in **figure 9** is considered, it is obvious that with not-vanishing displacement  $x$ , as defined in **figure 9**, the van der Waals interaction will have a tangential component, which would hinder also mode II or III displacements.

In order to estimate these shear stresses,  $\sigma_{xz}$ , the van der Waals forces between discrete atoms in certain regions were added numerically. The results of the discrete model for  $\sigma_{zz}$ , and  $\sigma_{xz}$  are shown in **figure 7**.  $\sigma_{zz}$  is always larger in the discrete model than in the continuum model since, in the former one, the minimum separation of the atoms is  $D$ , whereas in the continuum model the centers of the volume elements, which replace the atoms, are  $D + b$  apart.

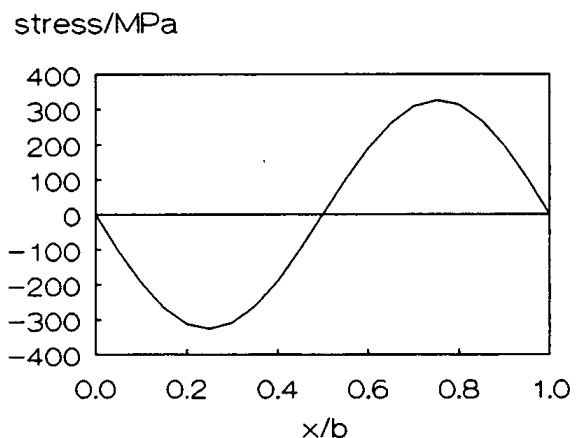


**Figure 10.** Variation of the shear stress  $\sigma_{xz}$  with  $x$ . The  $y$ -dependence is weak. Here  $y = 0$ ,  $D = b$

**Bild 10.** Variation der Schubspannungen  $\sigma_{xz}$  mit  $x$ . Die  $y$ -Abhängigkeit ist schwach. Hier ist  $y = 0$ ,  $D = b$

The most important result is, however, that the shear stresses,  $\sigma_{xz}$ , are much smaller than the normal stresses at any distance. **Figure 10** shows the dependence of  $\sigma_{xz}$ , on the lateral displacement,  $x$  (cf. **figure 9**) for  $y = 0$  and  $D = b$ . Their  $y$  dependence is rather weak (10% at  $D = 1.5b$  and 0.8% at  $D = 2.5b$ ). Even weaker are the  $x$ - and  $y$  dependences of  $\sigma_{zz}$  (1.2% at  $D = 1.5b$  and 0.01 % at  $D = 2.5b$ ). These results show the following: even if the atomistic structure of the interacting crack surfaces is fully taken into account, the van der Waals interaction produces strong normal forces and much weaker

tangential forces. Therefore, the conclusion is still valid that van der Waals interaction between crack surfaces hinders mode I opening of a crack, but has negligible effect on mode II or III shear displacements. A quantitative estimate of the effect of van der Waals stresses on crack growth behaviour requires some reasonable estimate of the distribution of the D-values as sketched in figure 8. Furthermore, a quantitative modelling of the interaction at the contact areas is required as well. Since both are not available yet, a quantitative model of these effects is out of reach still.

## Conclusions

1. The crack initiation mechanism may determine the growth behaviour of small cracks: slip band cracks in ferritic steels are hindered considerably at the first grain boundary, whereas twin boundary or triple point cracks in austenitic steels grow rather continuously.

2. In low strength materials the crack growth data become more transparent if plotted against the cyclic J integral: the explicit dependences on load amplitude, mean stress and crack length are reduced.

3. Crack closure of small cracks occurs in the austenitic steel at  $\sigma_{min}$ , because of mean stress relaxation at the crack tip. Premature closure occurs at cracks of medium length and is due to fracture surface roughness.

4. The opening stress is always markedly higher than the closing stress, which implies attractive interactions of the crack faces after closure.

5. Even if the effect of closure on crack growth is taken into account, cracks which are smaller than three grains, grow faster than longer cracks. This must be attributed to the favourable conditions for crack growth near crack initiation sites.

6. Closed small cracks will have a local COD of a few lattice constants over a large fraction of the total crack area. In these places van der Waals interactions produce attractive forces between crack faces as high as several hundred MPa.

7. Discrete summation of the van der Waals forces between atoms show, that high normal but only negligible tangential forces act between crack faces. Hence, van der Waals interactions hinder mode I but not mode II or III crack displacements. This may be the reason for the existence of the stage I crack growth regime.

## Acknowledgement

Partial financial support by the Deutsche Forschungsgemeinschaft under contract No.Rie 329/11-1 is gratefully acknowledged. (A 00 468; received: 19. Mai 1990)

## References

- 1) Lankford, J.: Engng. Frac. Mech. 9 (1977), p. 617/24.
- 2) Heitmann, H. H.; Vehoff, H.; Neumann, P.: [In:] "Advances in Fracture Research '84-Proc. ICF6", Vol. 5 (1984) [eds:] S. R. Valluri et al., Pergamon Press, Oxford and New York, p. 3599/3606.
- 3) Miller, K. J.: [In:] "Fundamentals of Deformation and Fracture", [eds:] B. A. Bilby et al., Cambridge University Press (1984), p. 477/500.
- 4) Raju, I. S.; Newman, J. C.: Engng. Frac. Mech. 11 (1979), p. 817/29.
- 5) Sharpe, W. N.: Int. J. Nondestructive Testing 3 (1971), p. 59/76.
- 6) Weiss, B.; Stickler, R.; Fathulla, A.: [In:] "Small Fatigue Cracks", [eds:] R. O. Ritchie, J. Lankford, The Metallurgical Society Inc., Warrendale PA (1986a), p. 471/98.
- 7) Polak, J.; Klesnil, M.: [In:] "Fracture Control of Engineering Structures - Proc. ECF6", Vol. 3 (1986), [eds:] H. C. van Elst, A. Bakker, EMAS, Warley, UK, p. 1559/568.
- 8) Wuethrich, C.: Int. J. Fract. 20 (1982), p. R35/37.
- 9) Rieux, P.; Driver, J.; Rieu, J.: Acta Met. 27 (1979), p. 145/53.
- 10) Dowling, N. E.; Begley, J. A.: [In:] "Mechanics of Crack Growth", ASTM STP 590 (1976), p. 82/101.
- 11) Rie, K. T.; Schubert, R.: [In:] "Low-Cycle Fatigue and Elasto-Plastic Behaviour of Materials", [ed:] K. T. Rie, Elsevier Applied Sciences, London and New York, 1987.
- 12) Iyyer, N. S.; Dowling, N. E.: [In:] "Small Fatigue Cracks", [eds:] R. O. Ritchie, J. Lankford, The Metallurgical Society Inc., Warrendale PA (1986), p. 213/23.
- 13) Rice, J. R.: [In:] "Fatigue Crack Propagation", ASTM STP 415 (1967), p. 247/309.
- 14) Lee, J. J.; Sharpe, W. N.: [In:] "Small Fatigue Cracks", [eds:] R. O. Ritchie, J. Lankford, The Metallurgical Society Inc., Warrendale PA (1986), p. 323/39.
- 15) Lankford, J.; Davidson, D. L.; Chan, K. S.: Met. Trans. 15A (1984), p. 1579/88.
- 16) Morris, W. L.; Buck, O.: Met. Trans. 8A (1977), p. 597/601.
- 17) Larsen, J. M.; Nicholas, T.; Thompson, A. W.; Williams, J. C.: [In:] "Small Fatigue Cracks", [eds:] R. O. Ritchie, J. Lankford, The Metallurgical Society Inc., Warrendale PA (1986), p. 499/512.
- 18) Suresh, S.; Ritchie, R. O.: Int. Metals Review 29 (1984), p. 445/78.
- 19) Budiansky, B.; Hutchinson, J. W.: J. Appl. Mech. 45 (1978), p. 267/76.
- 20) Fuhlrott, H.; Neumann, P.: Proc. Mechanisms of Environment Sensitive Cracking of Materials, Guilford, England (1977), p. 375.
- 21) Cook, R. F.; Fairbanks, C. J.; Lawn, B. R.; May, Y.-W.: J. Mat. Res. 2 (1987), p. 345.
- 22) Isrealachvili, J. N.: Intermolekular and Surface Forces, Academic Press, London, 1985.